Section 9

Development of and studies with coupled ocean-atmosphere models

Towards an integrated marine Arctic prediction system for METAREAs

[*]Hal Ritchie, Meteorological Research Division, EC, Dartmouth NS,
Gregory Smith, Meteorological Research Division, EC, Dorval QC
Christiane Beaudoin, Meteorological Research Division, EC, Dorval QC
Mark Buehner, Meteorological Research Division, EC, Dorval QC
Serge Desjardins, Meteorological Service of Canada – Atlantic, EC, Dartmouth NS
Pierre Pellerin, Meteorological Research Division, EC, Dorval QC
Charles-Emmanuel Testut, Mercator-Océan, Toulouse, France
Gilles Garric, Mercator-Océan, Toulouse, France

With the ever-increasing interest in resource exploitation and marine transport in the Arctic there is a mounting need for improved knowledge about the current and future environmental conditions in the Arctic. This need can be met by a new tri-ministerial initiative called the Canadian Operational Network of Coupled Environmental PredicTion Systems (CONCEPTS) among Environment Canada (EC), Fisheries and Oceans Canada (DFO), and the Department of National Defence (DND). CONCEPTS, in close collaboration with the French operational oceanographic centre Mercator-Océan, is providing a framework for research and operations on coupled atmosphere-ice-ocean prediction in Canada. Operational activity in CONCEPTS is based on coupling the Canadian atmospheric GEM (Global Environmental Multi-scale) model with the Mercator ice-ocean forecasting system based on the Nucleus for European Modelling of the Ocean (NEMO) ice-ocean model. The Mercator data assimilation system is based on a multi-variate SEEK data assimilation method that assimilates sea level anomaly, sea surface temperature (SST) and in situ temperature and salinity data. Using the Mercator forecasting system, weekly 1/4° resolution global 10-day ice-ocean forecasts are now being produced as well as daily 10-day forecasts at 1/12° resolution for the Northwest Atlantic. Ice fields are initialized using a 3DVAR ice analysis system that assimilates the manual ice analyses from the Canadian Ice Service, RadarSAT manual analyses as well as AMSR-E data. In addition, a high-resolution regional forecasting system for the Arctic is also under development. This system is initialized using 3DVAR ice analyses on a 5km North American grid (including the western Arctic) and produces daily 48hr ice forecasts.

In December 2007 Canada accepted official designation as the Issuing Service for meteorological Marine Safety Information (MSI) in the form of forecasts / warnings and ice bulletins for METAREAs XVII and XVIII (covering roughly the Beaufort Sea and the Canadian Arctic Archipelago up to the north pole; http://weather.gmdss. org/ metareas.html) as part of the Global Maritime Distress and Safety System (GMDSS). An important part of Environment Canada's involvement is the development of an integrated marine Arctic prediction system and satellite products in support of monitoring and

---

[*] *Corresponding author address*: Harold Ritchie, Environment Canada, 45 Alderney Drive, Dartmouth NS, Canada B2Y 2N6; E-mail: Harold.Ritchie@ ec.gc.ca

warnings. The integrated marine Arctic prediction system will feed into a highly automated information dissemination system. In particular, the METAREAs project objectives include the development, validation and implementation of marine forecasts with lead times of 1 to 3 days using a regional high resolution coupled multi-component (atmosphere, land, snow, ice, ocean and wave) modelling and data assimilation system to predict near surface atmospheric conditions, sea ice (concentration, pressure, drift, ice edge), freezing spray, waves and ocean conditions (temperature and currents). The core of the system will be an Arctic extension of the highly successful Gulf of St. Lawrence (GSL) coupled modelling system, with the GEM model as the atmospheric component coupled to the ice-ocean model. An ice-ocean data assimilation system is being developed in collaboration with Mercator-Océan using their SAM2 system for ocean data assimilation together with the 3DVAR ice analysis system developed at EC. The METAREAs research and development is a cornerstone activity within CONCEPTS.

An initial step toward the full coupled prediction system is the development of a stand-alone sea ice forecasting system. To investigate the potential skill of such a system, a simple forecasting system has been constructed based on the sea ice model from the coupled GSL forecasting system on the 5km North American grid used by the 3DVAR ice analysis system. To aid in the identification of sources of forecasting skill, two sets of forecasts have been produced: one with the thermodynamics activated in the model and a second without thermodynamics. As such, in the latter there is no formation or melt of sea ice; only the effects of ice advection and deformation due to wind forcing are included. This Sea Ice Forecasting System is running daily at the Canadian Meteorological Centre forced by forecasts from the Regional Deterministic Prediction System (RDPS). Ice forecasts are initialized using the 3DVAR North American sea ice analyses. Verification against Canadian Ice Service daily ice charts for the Eastern Arctic demonstrates that, by allowing the ice field to evolve based on model dynamics forced only by the winds, a modest gain can be obtained on a 24hr timescale as compared to persistence of analyses. When the Arctic is undergoing a period of ice formation, a significant further gain in ice forecasting skill is also obtained by activating thermodynamic processes in the ice model.

Development work is underway within the METAREAs project to couple the ice-ocean model to the GEM atmospheric model. Inclusion of an active ocean component will benefit the sea ice forecasts through a better representation of the role of tides in the development and maintenance of both sensible and latent heat polynyas as well as on ice drift and deformation. Following the benefits seen in the GSL (Faucher et al., 2010), a full atmosphere-ice-ocean coupling is expected to lead to further improvement in ice forecasting skill through the inclusion of a range of coupled processes. In particular, the large heat fluxes that occur across rapidly changing leads and polynyas have a large impact on the atmosphere and can lead to strong feedbacks through the winds and sea ice.

Reference

Faucher, M., F. Roy, H. Ritchie, S. Desjardins, C. Fogarty, G. Smith and P. Pellerin, 2010: "Coupled Atmosphere-Ocean-Ice Forecast System for the Gulf of St-Lawrence, Canada", Mercator Ocean Quarterly Newsletter, #38, July 2010, Laurent Crosnier editor, http://www.mercator-ocean.fr/documents/lettre/lettre_38_en.pdf, pages 23-37.

Preliminary case-study experiments with a global ocean-atmosphere coupled model configuration on NWP timescales

Ann Shelly, Tim Johns, Dan Copsey, Catherine Guiavarc'h
Met Office, Fitzroy Rd, Exeter, EX1 3PB, United Kingdom
(Email: ann.shelly@metoffice.gov.uk)

1. Introduction

A recent international workshop on ocean-atmosphere interaction held at the Met Office (Dec 2009), reviewed the current state of knowledge based on world-wide research activities in the field and set the background for the ongoing research in the Met Office. In bringing the community working actively in this area together to discuss the latest research, this workshop sought to identify which aspects of upper ocean-atmosphere interaction need to be included and what level of modelling complexity and initialization methods are most appropriate for different prediction timescales in global model systems for NWP through medium range to seasonal and decadal forecasting. It was decided to explore the potential for ocean-atmosphere coupling to deliver improved skill on NWP to monthly forecasting timescales.

2. Experimental design

A preliminary series of coupled atmosphere-ocean-sea ice experiments has been completed using a Met Office Unified Model (MetUM) configuration. In planning the initial research phase, the choice of ocean model configuration was of primary concern. A major strategic consideration was to move as close as possible towards scientific traceability between NWP forecast, seasonal and climate models, which are starting to converge within the MetUM environment. Thus the initial experiments were based on coupling to a fully 3-dimensional ocean model (NEMO) closely related to that used in Met Office seasonal forecast and climate model applications. In addition to coupled experiments, parallel atmosphere and ocean (including sea ice) control configurations were also developed and run. These were configured with identical physics and resolution and initialised in a similar way to the coupled experiments. In combination, this set of experiments permits the benefit from including the interactive ocean model and air-sea interactions to be analysed relatively cleanly.

The experimental setup is summarised in Table 1. A set of 6 winter (DJF) and 6 summer (JJA) test cases were chosen to correspond to the FOAM (ocean forecast model) hindcast period (2007-2008). Each case was run in forecast mode for 30 days as a standalone MetUM job, the cases being run separately for the coupled, atmosphere and ocean configurations.

3. Results

Figure 1 depicts the growth of Root Mean Square Error (RMSE) over the 30 day forecast period for the coupled and atmosphere control runs as compared with the MetUM analyses averaged over 6 winter cases for the global region (surface temperature). It suggests that the initial configuration of the experimental coupled model configuration compares favourably in terms of skill with atmosphere control run, with more skill than the control in the tropical region (not shown).

Initial results demonstrate relatively consistent biases and drifts compared to other Met office models such as FOAM and GloSea4 (coupled seasonal forecast model).Figure 2 shows that the coupled configuration, ocean control and GloSea4 all demonstrate similar SST drift in the Arabian sea compared with the FOAM analysis. Figure 3 shows mean GloSea4 DJF biases compared with day 5 coupled forecast errors. An equatorial cold tongue, Maritime Continent warm bias and cold Arabian Sea bias are visible at early lead times and further worsen with lead time.

4. Concluding remarks

The preliminary results are promising and work is underway to understand the mechanisms involved. This initial study contributes to the development of a seamless approach to weather, seasonal and climate forecasting, using the shorter range 1-15 day timescale to explore coupled model errors that are potentially important on the longer timescale.

Table 1: Outline of experimental setup for the coupled, atmosphere and ocean forecasts. Model sub-components are denoted **A** – atmosphere, **O** – ocean and **I** – sea ice

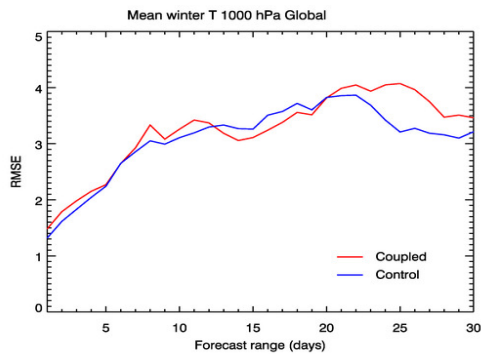|	**Coupled**	**Atmosphere control**	**Ocean control**
Components and resolution	**A** – MetUM N216L85 **O** – ORCA 0.25° L50 **I** – CICE 0.25°	**A** – MetUM N216L85	**O** – ORCA 0.25° L50 **I** – CICE 0.25°
Air-sea boundary conditions	Interactively coupled every 3 hours (resolving diurnal cycle)	Daily SST and sea ice from OSTIA analyses, time-interpolated to 3-hourly (but without a diurnal cycle)	3-hourly mean fluxes from corresponding atmosphere control
Initialisation	**A** - operational NWP analysis (N320L50), interpolated to N216L85 **O** - FOAM analysis (ORCA0.25L50) **I** - Monthly mean climatology from HadGEM3 pre-industrial control run	**A** - operational NWP analysis (N320L50), interpolated to N216L85	**O** - FOAM analysis (ORCA0.25L50) **I** - FOAM sea ice analysis

Figure 1: Mean DJF temperature rmse for coupled and atmosphere control runs calculated against MetUM analysis over Global region
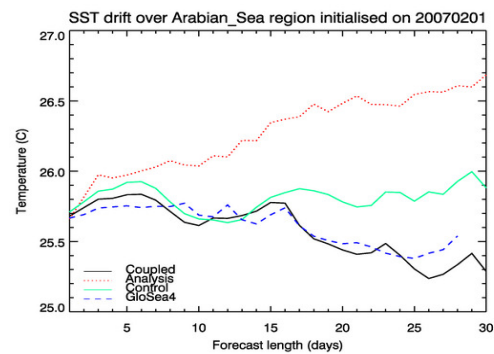

Figure 2: SST drift in Arabian Sea region for the coupled run, ocean control, GloSea4 and FOAM operational analysis for a single case study initialised on the 01/02/2007
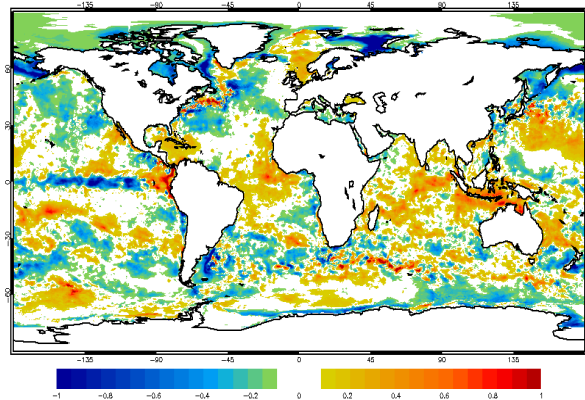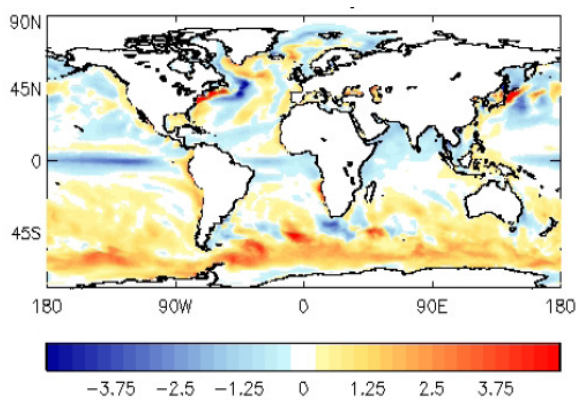

Figure 3: Mean Glosea4 DJF SST biases calculated against climatology (left). Mean DJF coupled model forecast errors at day 5 lead time calculated against FOAM operational analysis (right).

Impacts of short-term variation in sea-surface temperature and the sea state on the evolution of stationary tropical-cyclone-like vortex

Akiyoshi Wada*

*Meteorological Research Institute, Tsukuba, Ibaraki, 305-0052, JAPAN
awada@mri-jma.go.jp

1. Introduction

Previous studies reported that tropical-cyclone (TC) induced sea-surface cooling (SSC) directly affect the intensification and maximum intensity of a TC (Wada, 2009). However, the impact of short-term variation in sea-surface temperature (SST) such as diurnally-varying SST on TC intensification and its maximum intensity has not been investigated in detail so far. In addition, sea states varied at a short time scale are known to play a crucial role in determining exchange coefficients for momentum, sensible and latent heat fluxes. Sea states also enable to affect vertical turbulent mixing in the oceanic mixed layer due to breaking surface waves. Thus, variation in sea states can be considered as a crucial factor affecting TC intensification and its maximum intensity. This study addresses impacts of diurnally-varying SST (or noisy SST variation) and sea states on the development and maximum intensity of TC-like vortex using an atmosphere-wave-ocean coupled model (Wada et al., 2010).

2. Experiment design

The specification of the present numerical experiment is almost the same as Wada and Niino (2008) and Wada (2009) except that 1) an atmosphere-wave-ocean coupled model (Wada et al., 2010) is used instead of a nonhydrostatic atmosphere model coupled with mixed-layer ocean model, 2) integration time is 96 hours (h), not 81 h, 3) SST at the initial time is 30°C and 4) the coupled run begins from the initial time.

The formulation of Schiller and Godfrey (2005) (hereafter SG) with a short-wave absorption/penetration scheme of Ohlmann and Siegel (2000) is incorporated into the atmosphere-wave-ocean coupled model in order to calculate skin temperature in the vicinity of sea surface. The abbreviation 'SG' indicates the inclusion of the Schiller and Godfrey scheme into the coupled model. In order to investigate the significance of the impact of diurnally-varying SST on TC intensification and its maximum intensity, we perform the numerical experiments in TY and TYSG (Table 1) and the other numerical experiments given uniform random real numbers in the interval (0, 0.1] generated using the multiplicative congruence method. How to provide random noises to calculated SST is presented in Table 1.

Table 2 shows what roughness-length scheme is used for each numerical-prediction experiment. The roughness length derived from Taylor and Yelland (2001) is based on wave steepness. The roughness length derived from Kondo (1975) is based on the dependency of 10-m wind speed.

Table 1 Abbreviations of numerical-prediction experiments, method of SST variation, and scheme of roughness length. The character '-' means an experiment without using an oceanic sublayer scheme (Schiller and Godfrey, 2005).

EXP.	SST VARIATION	Roughness Length
TY	–	Taylor and Yelland(2001)
TYSG	Schiller and Godfrey (2005)	Taylor and Yelland(2001)
TYPP	$+0 - 0.1^{\circ}$C overall the area	Taylor and Yelland(2001)
TYZZ	$-0.05 - +0.05^{\circ}$C overall the area	Taylor and Yelland(2001)
TYMM	$-0.1 - 0^{\circ}$C overall the area	Taylor and Yelland(2001)
TYLP	$+0 - 0.1^{\circ}$C where the amplitude in SG $> 0.1^{\circ}$C	Taylor and Yelland(2001)
TYLZ	$-0.05 - 0.05^{\circ}$C where the amplitude in SG $> 0.1^{\circ}$C	Taylor and Yelland(2001)
TYLM	$-0.1 - 0^{\circ}$C where the amplitude in SG $> 0.1^{\circ}$C	Taylor and Yelland(2001)

Table 2 Same as Table 1.

EXP.	SST VARIATION	Roughness Length
TY	–	Taylor and Yelland(2001)
KD	–	Kondo(1975)
CH	–	Charnock(1955)
JA	–	Janssen(1991)
SM	–	Smith(1992)

The roughness length derived from Charnock (1955) is based on the constant value of the ratio of gravity acceleration multiplied roughness length to frictional velocity squared. Janssen (1991) proposed the formulation of roughness length that the Charnock constant value varied depending on the ratio of wave-induced stress to wind stress, while Smith et al. (1992) proposed it that the Charnock constant value varied depending on the ratio of frictional velocity to the wave age. It should be noted that the impact of diurnally-varying SST on TC intensification and its maximum intensity is investigated only by the atmosphere-wave-ocean coupled model with the roughness length scheme of Taylor and Yelland (2001), while the impact of sea states is investigated by the atmosphere-wave-ocean coupled model without the inclusion of the Schiller and Godfrey scheme.

3. Results

The evolutions of central pressures (CPs) of TC-like vortex calculated by the atmosphere-wave-ocean coupled model with the SG scheme or various SST noises (Table 1) are shown in Figs. 1 and 2. TC-like vortex undergoes slow intensification from 0 h to 24 h and the vortex turns to experience rapid intensification to 48 h in all numerical experiments. Then the vortex gradually weakens due to SSC. The range of SSC defined as a decrease in SST from the initial time is -6.8 to -7.9 °C at 96 h. The minimum value of a decrease in SST from the initial time is -8.0 to -8.6 °C occurred while the vortex gradually weakens at the mature phase.

A difference in CPs between TY and TYSG is comparable to that between TY and the other numerical experiments given various SST noises. This result indicates that the impact of diurnally-varying SST on the evolution of CP is regarded as the impact of noisy SST variation on it when TC-like vortex is stationary. The impact of noisy SST variation is remarkable from 36 h to 48 h in TYSG, TYZZ, TYMM, TYLP and TYLM corresponding to the rapid intensification phase. The impact of noisy SST variation is independent of the area of noisy SST variation whether it is overall the computational domain or limited where the amplitude of skin temperature is greater than 0.1 °C.

In contrast, a difference of roughness-length schemes shown in Table 2 directly affects the evolution of CP from 24 h to 48 h, corresponding to the rapid intensification phase, while the difference turns to be relatively small after 48 h, corresponding to the mature phase of TC-like vortex. This reveals that roughness length plays a crucial role in rapidly intensifying TC-like vortex. This phase corresponds to eye-eyewall mixing process inside the eyewall. Mesovortices appear within the core of TC-like vortex and they are merged into a vorticity ring during the phase.

In summary, rapid intensification is affected by surface friction changed by roughness-length schemes at the early rapid intensification phase, while it is also affected by noisy SST variation, including diurnally-varying SST, at the late rapid intensification phase.
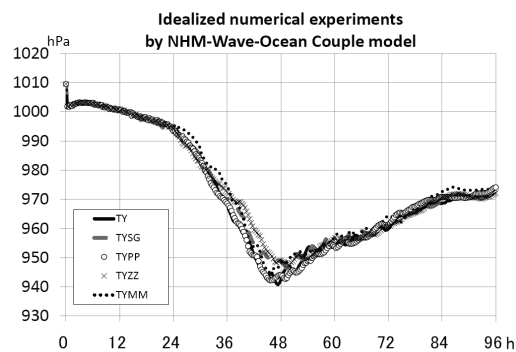

Figure 1 Time series of simulated central pressure of TC-like vortex in TY, TYSG, TYPP, TYZZ and TYMM (Table 1).
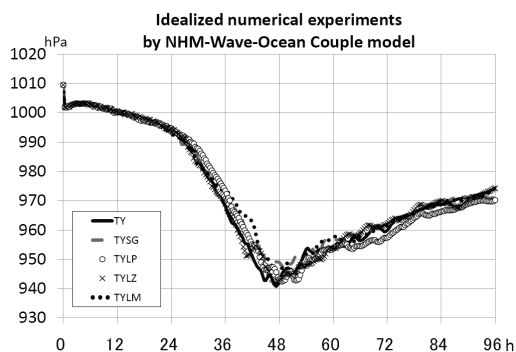

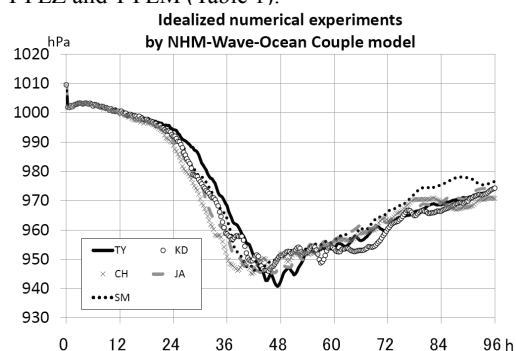Figure 2 Same as Fig. 1 except in TY, TYSG, TYLP, TYLZ and TYLM (Table 1).

Figure 3 Same as Fig. 1 except in TY, KD, CH, JA and SM (Table 2).

References

Charnock, H. (1955): Wind stress on a water surface. *Quart. J. Roy. Meteorol. Soc.*, **81**, 639-640.

Janssen, P. A. E. M. (1991): Quasi-linear theory of wind-wave generation applied to wave forecasting. *J. Phys. Oceangr.*, **21**, 1631-1642.

Kondo, J. (1975): Air-sea bulk transfer coefficients in diabatic conditions, *Boundary Layer Meteorol.*, **9**, 91-112.

Ohlmann, J. C. and D. A. Siegel (2000): Ocean radial heating. Part II: Parameterizing solar radiation transmission through the upper ocean. *J. Phys. Oceanogr.*, **30**, 1849-1865.

Schiller, A. and J. S. Godfrey (2005): A diagnostic model of the diurnal cycle of sea surface temperature for use in coupled ocean-atmosphere models. *J. Geophys. Res.*, **110**, C11014.

Smith, S. D., R. J. Anderson, W. A. Oost, C. Kraan, N. Maat, J. DeCosmo, K. B. Katsaros, K. L. Davidson, K. Bumke, L. Hasse and H. M. Chadwick (1992): Sea surface wind stress and drag coefficients: The HEXOS results. Boundary-Layer Meteorol., 60, 109-142.

Taylor, P. K., and M. J. Yelland (2001): The dependence of sea surface roughness on the height and steepness of the waves. *J. Phys. Oceanogr.*, **31**, 572–590.

Wada, A. and H. Niino (2008): Numerical experiments of intensification of an idealized typhoon-like vortex under various sea surface temperatures by a nonhydrostatic atmosphere-ocean coupled model. CAS/JSC WGNE Research Activities in Atmosphere and Oceanic Modelling, 0905-0906.

Wada, A. (2009): Idealized numerical experiments associated with the intensity and rapid intensification of stationary tropical cyclone-like vortex and its relation to initial sea-surface temperature and vortex-induced sea-surface cooling. *J. Geophys. Res.*, **114**, D18111.

Wada, A., N. Kohno and Y. Kawai (2010): Impact of wave-ocean interaction on typhoon Hai-Tang in 2005. *SOLA*. **6A**. 13-16.

Drag coefficient under extremely high winds of typhoon Hai-Tang (2005)

Akiyoshi Wada*

*Meteorological Research Institute, Tsukuba, Ibaraki, 305-0052, JAPAN
awada@mri-jma.go.jp

1. Introduction

Sea states at the interface between the atmosphere and the ocean play a crucial role in calculating air-sea exchange coefficients for momentum, heat and moisture fluxes. Breaking surface waves occurred at the interface underneath a tropical cyclone (TC) result in variations in sea states and then TC-induced sea-surface cooling (SSC) due to an increase in turbulent kinetic energy near the surface (Wada et al., 2010). SSC leads possibly to reduce turbulent heat and moisture fluxes in the vicinity of the center of a TC due to a small difference in air-sea temperatures and moistures. The reduction in the fluxes is responsible for slower intensification and changes in inner-core eye-eyewall mixing processes at the intensification phase.

This report addresses the other aspect of sea states on TC intensification. That is a role of surface friction in TC intensification through changes in oceanic roughness lengths, frictional velocities, and drag coefficients (C_d). Recent studies indicated that C_d leveled off at very high wind speed (30 to 40 m s^{-1}) (Powell et al., 2003; Donelan et al., 2004), while the average of enthalpy coefficients (C_k) seems to keep constant up to 30 m s^{-1}. When C_k keeps constant at the very high wind speed, the ratio (C_k/C_d) turns to increase due to a decrease in C_d. According to 'Wind-Induced Surface Heat Exchange' mechanism proposed by Emanuel (1995), high C_k/C_d provides a favorable condition for forming a stronger TC with high maximum potential intensity. The purpose of this report is therefore to investigate effects of sea states on TC intensity predictions using an atmosphere-wave-ocean coupled model developed by the author.

2. Experiment design

The atmosphere-wave-ocean coupled model consists of a nonhydrostatic atmosphere model (NHM) developed at the Japan Meteorological Agency (JMA) and Meteorological Research Institute (MRI), the third generation ocean wave model for operational developed at the JMA and mixed-layer ocean model developed at the MRI (Wada et al., 2010). It should be noted that the effect of breaking surface waves on an entrainment at the mixed-layer base is incorporated into the mixed-layer ocean model (Wada et al., 2010).

The computational domain of the coupled model is 4320 km in the longitudinal direction and 2520 km in the meridian direction with the horizontal grid spacing of 3 km. The time step of NHM is 8 s, that of the mixed-layer ocean model is 48 s and that of the ocean wave model is 600 s. NHM has 40 vertical levels, and the interval between levels varies from 40 m near the surface to 1180 m for the uppermost layer. The model top height of NHM is nearly 23 km. The number of layers in the mixed-layer ocean model is four, which is the same as Wada et al. (2010). Oceanic initial conditions are obtained from daily oceanic reanalysis data in 2005 with a horizontal grid spacing of 0.5°, calculated by the MOVE system (Usui et al., 2006).

The specification of the coupled model is as follows. No convective parameterization scheme is used. The roughness length is estimated by Taylor and Yelland (2001). Two kinds of numerical simulations are carried out (Table 1): one uses a scheme of Louis et al. (1982) for determining exchange coefficients, which is based on the Monin-Obukhov similarity theory (hereafter TYL). The other uses a scheme of Kondo (1975), assuming the dependency of exchange coefficients on surface wind speed (hereafter TYK).

To set the initial and boundary atmospheric conditions, a hydrostatic global spectral model (GSM) version T213L40 with a horizontal grid spacing of nearly 60 km was previously run for 72 h. To avoid gaps in the horizontal resolution of downscale calculations, a hydrostatic regional spectral typhoon model (TYM) with a horizontal grid spacing of nearly 20 km was subsequently run for 72 h as a preparation. The TYM provides initial and boundary atmospheric conditions every 3 h to the coupled model. The integration time of GSM, TYM and the coupled model in TYL and TYK is 72h, starting from 1200 UTC 1 July 2005.

Table 1 Designations of the numerical-prediction experiments and surface boundary processes (roughness lengths and exchange coefficients) used to conduct the experiments.

Experiments	Surface boundary processes	
	Roughness lengths	Exchange coefficients
TYL	Taylor and Yelland (2001)	Louis et al (1982)
TYK	Taylor and Yelland (2001)	Kondo(1975)

3. Results

Predicted central pressures (CPs) are compared to best-track CP archived by the Regional Specialized Meteorological Center Tokyo-Typhoon Center (Fig.1a). Relatively low predicted CPs compared to best-track CP are similar results to Wada et al. (2010). The evolution of best-track CP indicates intensification from 12 h to 36 h, while the evolutions of predicted CPs indicate little intensification. A difference in surface boundary schemes between TYL and TYK hardly affects a northwestward track error reported in Wada et al (2010) (not shown).

A difference in predicted CPs between TYL and TYK begins to appear clearly after 36 h. A rapid decrease in the predicted CPs from 36 h to 72 h indicates rapidly intensification, which is partly seen in best-track CP (60 h to 72 h). The predicted CP in TYK is lower than that in TYK during the period. The predicted CP in TYK is lower than that in best-track CP at 72 h, while the predicted CP in TYL is higher than that in best-track CP.

As 10-m wind is higher, C_d is usually high when some bulk formulas (e.g. Kondo, 1975) are used for the estimate of C_d. The result in this report, however, shows that C_d levels off at very high winds (higher than 40 m s^{-1}) with greater standard deviations. A difference in the values of C_d between TYL and TYK becomes clear when 10-m wind is higher than 40 m s^{-1}. C_d rapidly levels off in TYK, which is consistent with the observational result of Powell et al. (2003). In contrast, C_d tends to keep constant in TYL, similar to the experimental result of Donelan et al (2004).

A difference in dependencies of the ratio C_k/C_d on 10-m wind becomes clear when 10-m wind is higher than 50 m s^{-1} (Fig.2). The ratio calculated in TYK is higher than that calculated in TYL, implying that maximum potential intensity, proposed by Emanuel (1995), in TYK is stronger than that in TYL. This implication is consistent with the numerical-prediction result shown in Fig.1a.

4. Concluding remarks

A difference in surface boundary schemes incorporated into an atmosphere-wave-ocean coupled model results in a difference in the dependencies of C_d on 10-m wind particularly at very high winds. However, the values of C_d obtained in the present numerical predictions are relatively low compared with previous studies (e.g. Powell et al., 2003; Donelan et al, 2004). The couple model will be needed to be modified particularly in variations in roughness lengths such as a modification of the coefficients of the empirical formula of Taylor and Yelland (2001) in order to improve the estimate of the underestimation of C_d.
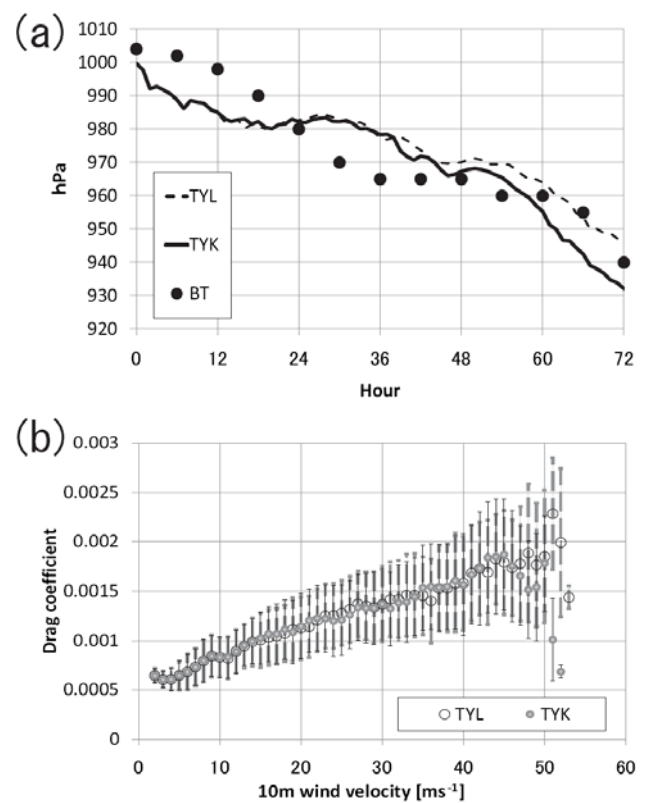

Figure 1 (a) Time series of best-track central pressure (CP), predicted CP in TYL and TYK, and (b) A scatter diagram of 10-m wind velocity and drag coefficient (C_d) in TYL and TYK at 72h.
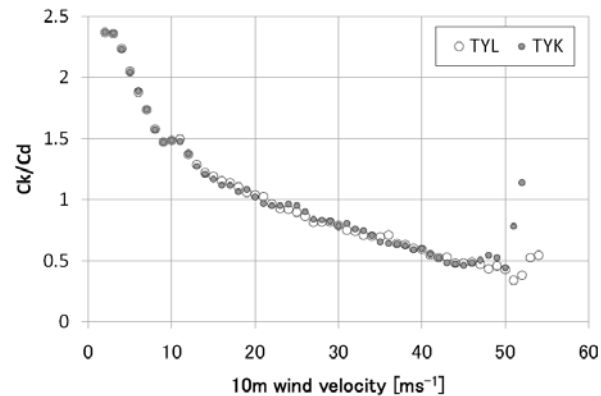

Figure 2 A scatter diagram of 10-m wind velocity and the ratio C_k/C_d in TYL and TYK.

References
Donelan, M. A., B. K. Haus, N. Reul, W. J. Plant, M. Stiassnie, H. C. Graber, O. B. Brown, and E. S. Saltzman (2004): On the limiting aerodynamic roughness of the ocean in very high winds, *Geophys. Res. Lett.*, **31**, L18306.
Emanuel, K. A. (1995): Sensitivity of tropical cyclones to surface exchange coefficients and a revised steady-state model incorporating eye dynamics. *J. Atmos. Sci.*, **52**, 3969–3976.
Kondo, J. (1975): Air-sea bulk transfer coefficients in diabatic conditions, *Boundary Layer Meteorol.*, **9**, 91-112.
Louis, J.F., M. Tiedtke, and J.F. Geleyn (1982): A short history of the operational PBL parameterization at ECMWF. Proc. *Workshop on Planetary Boundary Layer Parameterization*, Reading, United Kingdom, ECMWF, 59–79.
Powell, M. D., P. J. Vickery, and T. A. Reinhold (2003): Reduced drag coefficient for high wind speeds in tropical cyclones, *Nature*, **422**, 279-283.
Taylor, P. K., and M. J. Yelland (2001): The dependence of sea surface roughness on the height and steepness of the waves. *J. Phys. Oceanogr.*, **31**, 572–590.
Usui, N., S. Ishizaki, Y. Fujii, H. Tsujino, T. Yasuda, and M. Kamachi (2006): Meteorological Research Institute multivariate ocean variational estimation (MOVE) system: Some early results. *J. Adv. Space Res.*, **37**, 806–822.
Wada, A., N. Kohno and Y. Kawai (2010): Impact of wave-ocean interaction on typhoon Hai-Tang in 2005. *SOLA*. **6A**. 13-16.

Variation in air-sea CO_2 flux and pH induced by passage of typhoon Hai-Tang (2005)

Akiyoshi Wada*, Takashi Midorikawa and Masao Ishii

Meteorological Research Institute, Tsukuba, Ibaraki, 305-0052, JAPAN

*awada@mri-jma.go.jp

1. Introduction

Sudden variation in air-sea carbon dioxide (CO_2) flux has been studied from observational and numerical viewpoints so far. Air-sea CO_2 flux is usually calculated by empirical bulk formulas using gas transfer velocity (piston velocity) and a difference in partial CO_2 pressures (pCO_2) between the atmosphere and the ocean. The oceanic partial CO_2 pressure pCO_2^{sea} and the hydrogen ion concentration (usually reported by the normalization of pH to a temperature of 25ºC) can be diagnostically calculated by given water temperature, salinity, dissolved inorganic carbon (DIC) and total alkalinity(ALK). This report addresses the variation in pCO_2^{sea}, PH and air-sea CO_2 flux by passage of a tropical cyclone. A numerical experiment is performed to investigate the variations during the passage of typhoon Hai-Tang in 2005.

2. Experiment design

A simple chemical scheme (Wada et al., 2011) was incorporated into the atmosphere-wave-ocean coupled model (Wada et al., 2010). Initial conditions of DIC and ALK are provided from the empirical formulas derived from observations by research vessels (Wada et al., 2011). Water temperature and salinity at the initial time are provided from daily oceanic reanalysis data with a grid spacing of 0.5º calculated by the Meteorological Research Institute multivariate Ocean Variational Estimation system (MOVE) (Usui et al., 2006). The atmospheric partial CO_2 pressure pCO_2^{air} is assumed to be expressed as follows,

$$pCO_2^{air} = pCO_2^{sea}(t=0) - 20(ppm),\qquad(1)$$

where $pCO_2^{sea}(t=0)$ is pCO_2^{sea} at the initial time. A detail description of experiment design for the atmosphere-wave-ocean model is described in Wada et al. (2010). The specification of the coupled model is as follows. Oceanic roughness length is calculated based on Taylor and Yelland (2001). Exchange coefficients for momentum, heat and moisture fluxes are calculated by Kondo (1975).

3. Results

At the initial time, pCO_2^{sea} is 390 μ atom and almost horizontally uniform (Fig. 1a). At 72 h, pCO_2^{sea} is higher than that at the initial time along the track of predicted Hai-Tang particularly on the right side of the track from 144° to $148^{o}E$ (Fig. 1b), corresponding to less intensification phase. In contrast, pCO_2^{sea} decreases behind the center of predicted Hai-Tang around $136^{o}E$.

pCO_2^{sea} is relatively high along Hai-Tang's track where sea-surface temperature (SST) becomes low (Fig. 2a) and DIC becomes high (Fig. 2b). Relatively low SST and high DIC along the track of predicted Hai-Tang result from Hai-Tang-induced vertical turbulent mixing in the upper ocean. The effect of the vertical turbulent mixing on the increase in pCO_2^{sea} and DIC and the decrease in SST differs depending on the oceanic environment such as a horizontal distribution of mixed-layer depth at the initial time (Wada et al., 2010). Oceanic environments can affect not only the intensity prediction but also the chemical oceanic response to Hai-Tang. It should be noted that the oceanic environment at the initial time can also affect a horizontal distribution of DIC.
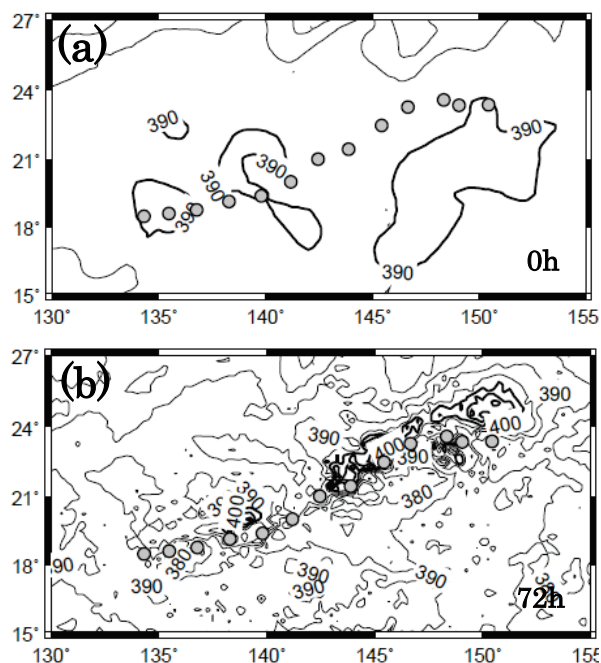

Figure 1 Horizontal distribution of predicted pCO_2^{sea} at (a) 0 h and (b) 72 h.

A horizontal distribution of PH at 72 h is shown in Fig. 3. PH clearly decreases from 144º to 148ºE on the right side of the track of predicted Hai-Tang. The area of low PH corresponds to the area of high pCO$_2$^{sea}, high DIC and low SST. This indicates that PH tends to become low when a mixed layer is thin underneath Hai-Tang. In other words, PH hardly decreases when Hai-Tang passes across warm-core eddies with horizontal scale of a few hundred kilometers. In addition, PH tends to easily decrease when Hai-Tang passes over the area where DIC is high and SST is relatively low.

After the passage of Hai-Tang, it is interesting that low PH remains around 24ºN, 148ºE where predicted Hai-Tang undergoes recurvature. This implies that surface-water acidification due to the passage of Hai-Tang is affected by moving speeds of Hai-Tang as well as oceanic environment. The process associated with low PH induced by Hai-Tang is similar to Hai-Tang-induced sea-surface cooling due to Ekman pumping and vertical turbulent mixing. The transport of cool water with low PH from a seasonal thermocline is efficiently mixed in the upper ocean at the recurvature phase and plays a crucial role in surface-water acidification.

Sea-to-air CO$_2$ flux is remarkable around the center of predicted Hai-Tang (Fig. 4). After the passage of Hai-Tang, CO$_2$ flux rapidly decreases due to a small $\triangle$ pCO$_2$ and weakening surface wind speed. It should be noted that there is still uncertainty in the gas transfer velocity under high winds.

Because there is little chemical observation around the area where Hai-Tang passed, it is difficult to validate the present numerical results. Chemical observations during the passage of a tropical cyclone (TC) will be needed to develop the present coupled model. This report proves that rapid increases in sea-to-air CO$_2$ flux occurs during the passage of TCs. The coupled model will contribute the estimate of the abrupt sea-to-air CO$_2$ flux on global carbon circulation.
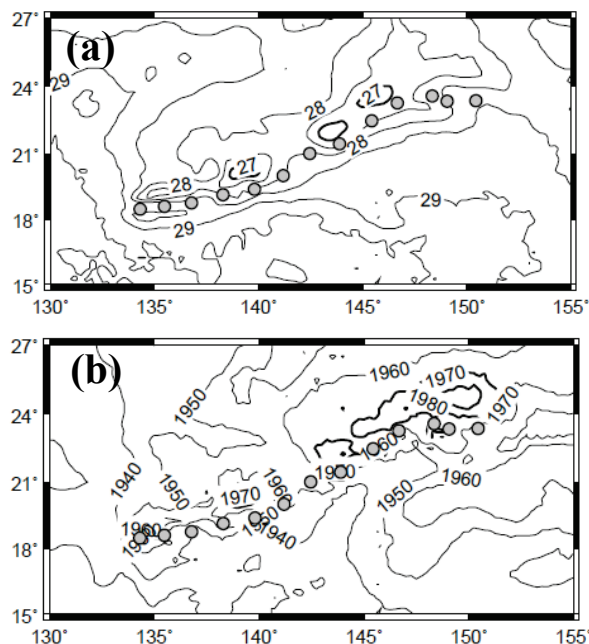

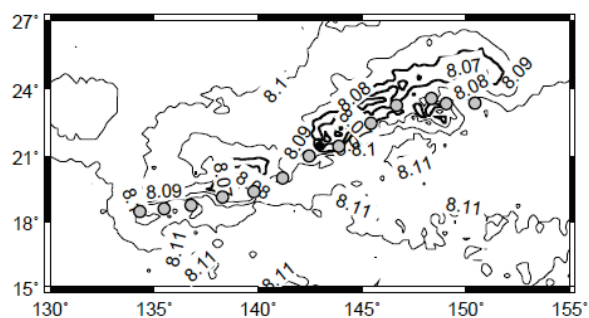Figure 2 Same as Figure 1 except for sea-surface temperature at 72 h and (b) DIC at 72 h.
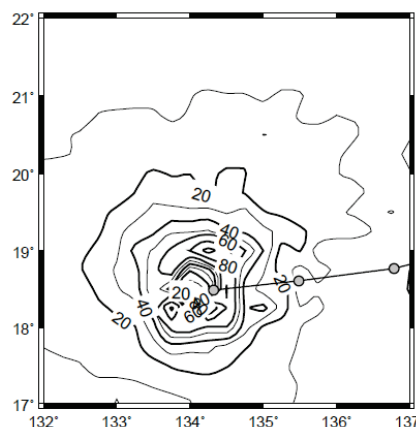

Figure 3 Same as Figure 1 except for PH at 72h.

Figure 4 Horizontal distribution of sea-to-air CO2 flux at 72h.

References
Kondo, J. (1975): Air-sea bulk transfer coefficients in diabatic conditions, *Boundary Layer Meteorol.*, **9**, 91-112.
Taylor, P. K., and M. J. Yelland (2001): The dependence of sea surface roughness on the height and of the waves. J. Phys. Oceanogr., 31, 572–590.
Usui, N., S. Ishizaki, Y. Fujii, H. Tsujino, T. Yasuda, and M. Kamachi (2006): Meteorological Research Institute multivariate ocean variational estimation (MOVE) system: Some early results. *J. Adv. Space Res.*, **37**, 806–822.
Wada, A., N. Kohno and Y. Kawai (2010): Impact of wave-ocean interaction on typhoon Hai-Tang in 2005. *SOLA*. **6A**. 13-16.
Wada, A., T. Midorikawa and M. Ishii (2011): Sudden decreases in pCO2 simulated by a simple chemical scheme during the passage of Tina and Winnie (1997). *CAS/JSC WGNE Res. Activ. Atmos. Oceanic Modell.* Submitted.